



The water vapor foreign continuum in the 8100–8500 cm⁻¹ spectral range

A.O. Koroleva^{a,b}, S. Kassia^a, D. Mondelain^a, A. Campargue^{a,*}

^a Univ. Grenoble Alpes, CNRS, LIPhy, Grenoble, France

^b Institute of Applied Physics of RAS, Nizhny Novgorod, Russia



ARTICLE INFO

Article history:

Received 5 October 2022

Revised 18 November 2022

Accepted 18 November 2022

Available online 25 November 2022

Keywords:

Water vapor

Foreign continuum

MT_CKD model

CRDS

Transparency window

Atmosphere

ABSTRACT

In the Earth's atmosphere, the foreign absorption continuum of water vapor is due to the interaction of water molecules with other atmospheric gases (mostly N₂ and O₂). Following our study of the self-continuum in the high energy edge of the 1.25 μm transparency window (Koroleva et al., J. Quant. Spectrosc. Radiat. Transfer 286 (2022) 108206), we report here the first room temperature measurements of water vapor foreign continuum in the same spectral region. Foreign continuum cross-sections, C_F , are derived at several selected spectral points between 8120 and 8500 cm⁻¹ for humidified nitrogen, humidified oxygen and humidified air (10000 ppm of H₂O). The absorption signal is measured by cavity ring-down spectroscopy (CRDS) using pressure ramps up to 750 Torr. While the measured total continuum absorption follows nicely the expected quadratic dependence *versus* the total pressure, the uncertainty on the retrieved weak foreign continuum is strongly affected by other contributions which have to be subtracted from the measured absorption (far wings of the resonance lines, O₂ collision induced absorption, self-continuum, Rayleigh scattering). The obtained H₂O-air and H₂O-N₂ C_F cross-section values are found to be comparable while the H₂O-O₂ C_F values appear to be significantly smaller. Overall, the retrieved C_F values for H₂O-air mixture validate the MT_CKD model in the considered region.

© 2022 Elsevier Ltd. All rights reserved.

1. Introduction

The absorption of light by water vapor includes two main contributions: the well-known narrow rovibrational absorption lines (or resonance spectrum) and a broad-band contribution with weak frequency dependence, the continuum. In the Earth's atmosphere, the continuum includes the self-continuum and the foreign continuum related to water molecules in interaction with one another or with other atmospheric species (mostly N₂ and O₂), respectively. As a result, the self-continuum varies as the square of the water vapor partial pressure, P_{H_2O} , while the foreign continuum is proportional to $P_{H_2O}P_F$ where P_F is the foreign gas pressure (dry air here). The water vapor absorption coefficient is thus expressed as:

$$\alpha_W(\nu, T) = \alpha_{WML} + \alpha_{WCS} + \alpha_{WCF}$$

$$= \alpha_{WML} + \frac{1}{kT} C_S(\nu, T) P_{H_2O}^2 + \frac{1}{kT} C_F(\nu, T) P_{H_2O} P_F \quad (1)$$

where α_{WML} , α_{WCS} and α_{WCF} are the contributions due to resonant lines (WML), the water vapor self-continuum (WCS) and the for-

foreign continuum (WCF), respectively. k is the Boltzmann constant, P_{H_2O} and P_F are the water vapor and foreign gas partial pressures, respectively (thus $P = P_{H_2O} + P_F$ where P is the total pressure). C_S and C_F are the self- and foreign continuum cross-sections expressed in cm²molecule⁻¹atm⁻¹.

Depending on the atmospheric conditions, the foreign continuum contribution to the absorption by water vapor can be of the same order as the self-continuum contribution which makes the characterization of both necessary. The semi-empirical MT_CKD (Mlawer–Tobin–Clough–Kneizys–Davies) model [1–3] is the standard model implemented in climate and weather prediction models to account for the water continuum. In the windows between absorption bands, this model is mostly a far-wing line shape model with parameters empirically adjusted according to laboratory or atmospheric data at disposal, mostly in the infrared (e.g. [3–5]). In the near-infrared, the original MT_CKD cross-sections (i.e. MT_CKD_1.0 through _3.0) thus result from long-range extrapolation which had to be validated.

Since 2013, we are involved in a long-term experimental project aiming to characterize the water vapor continuum mostly in the near-infrared windows where previous data were very scarce and reported with large uncertainties. Due to the weakness of the

* Corresponding author.

E-mail address: alain.campargue@univ-grenoble-alpes.fr (A. Campargue).

continuum signal, the measurements are performed using cavity enhanced absorption spectroscopy techniques (mostly cavity ring down spectroscopy - CRDS - but also optical feedback cavity enhanced absorption spectroscopy - OFCEAS) [7–17]. The cross-section values derived at specific spectral points are systematically used for validation tests of the current version of the MT_CKD model. Although a number of significant deviations were evidenced (e.g. the MT_CKD self-continuum in its 3.0 version was underestimated by a factor 5 to 10 near the centre of the 2.3 μm window [11–13,16]), the measurements roughly validated the MT_CKD values up to 8000 cm^{-1} [17]. Considering the long-range spectral extrapolation of this semi-empirical model, this achievement deserves to be underlined. The most recent versions of the MT_CKD self-continuum (from V3.2) were refined according to our CRDS and OFCEAS experimental cross-sections in the 4.0, 2.1, 1.6 and 1.25 μm windows [3].

As concerns the foreign continuum absorption, experimental data are scarcer [18], in particular at room temperature. In-band continuum measurements were reported in the 3500–4000 cm^{-1} spectral range by direct absorption spectroscopy [6], between 1300 and 7500 cm^{-1} by Fourier transform spectroscopy (FTS) [19] and in the 0.94 μm absorption band by CRDS [20]. Of interest for the present investigation in the 1.25 μm transparency window are the high temperature (350–430 K) foreign continuum FTS measurements by the CAVIAR consortium (Continuum Absorption at Visible and Infrared wavelengths and its Atmospheric Relevance) over the wide 1.1 – 5.0 μm spectral range thus including the 1.25 μm window of interest [21]. The comparison of the present room temperature measurements to the CAVIAR high temperature measurements might give insights on the temperature dependence of the foreign-continuum absorption which is known to be weak, much weaker than that of the self-continuum; the latter being known to decrease sharply with temperature.

In the transparency windows, measurements of the water foreign continuum are limited, in particular at room temperature, and spectrally dispersed. Cormier et al. [22] and Baranov&Lafferty [23] reported measurements in the 10 μm window by CRDS and FTS, respectively. The water foreign continuum was determined in the 4.0 μm window by FTS [23–25], in the 2.1 and 1.6 μm windows by CRDS [9,14,15] and near 14400 cm^{-1} by photoacoustic spectroscopy [26]. On the basis of Refs. [9,22], the MT_CKD foreign continuum has been significantly increased starting with version 2.8 [3].

To the best of our knowledge, no attempts were previously undertaken to measure the room temperature foreign continuum in the 1.25 μm window. Indeed, as described below the measurements are particularly demanding in this region due to the weak absorption signal to be measured and to the fact that the foreign contribution represents only a generally small fraction of the total measured absorption. In this situation, the derived foreign cross-section values are directly impacted by the evaluation of the other contributions (resonance lines broadened by N_2 , O_2 or dry air, O_2 collision induced absorption band near 1.27 μm , self-continuum absorption, Rayleigh scattering) which have to be subtracted from the measured CRDS absorption coefficient. In order to help disentangling the different contributions, different series of measurements were performed using as foreign gas, pure N_2 , pure O_2 and dry air. These three sets of derived C_F values will allow to test their self-consistency and discuss their uncertainties.

The remaining part of this paper is organized as follows: the data analysis is detailed in Section 3 after the description of the data acquisition in the next experimental section. In Section 4, we discuss the consistency of our results and compare them to the MT_CKD model [2,3] and to CAVIAR high temperature data [21].

2. Experimental

Water foreign continuum absorption measurements were performed by CRDS for a series of spectral points of the high energy edge of the 1.25 μm window (8105 – 8480 cm^{-1}). The data acquisition was performed at fixed frequency during pressure ramps of humidified gas (dry air, nitrogen and oxygen). The experimental approach is mostly the same as described in Ref. [17] for the self-continuum determination, except that the amplitude of the pressure ramps is much larger (up to 1 atm). The spectrometer uses an external cavity diode laser (ECDL, Toptica fiber-connected DL pro, 1200 nm) as a light source. About 10% of the light intensity is sent to a wavelength meter (HighFinesse WSU7-IR, 5 MHz resolution, 20 MHz accuracy over 10 hours) which provides the laser frequency. The main part of the radiation is injected into the 1.4 m long CRDS cavity using a single mode fiber. The coincidence between the laser frequency and that of one mode of the CRDS cavity is achieved by modulating the rear mirror of the cavity mounted on a piezoelectric transducer (PZT), over about half the wavelength, corresponding to the free spectral range of the cavity. At resonance, the cavity is filled with photons and then the injection of the laser light is interrupted by an acousto-optic modulator. An InGaAs PIN photodiode is used to measure the purely exponential decay time of photons leaking from the cavity. The absorption coefficient, $\alpha(\nu)$, is determined directly from fitted RD time, τ :

$$\alpha(\nu) = \frac{1}{c\tau(\nu)} - \frac{1}{c\tau_0(\nu)} \quad (1)$$

where c is the speed of light. τ_0 and τ correspond to the ring down time of the cavity empty and filled with gas, respectively.

In the present experiments, Rayleigh scattering has a non-negligible contribution to the increase of the loss rate, $\frac{1}{c\tau(\nu)}$. (For convenience, “absorption coefficient” will be used in the following to name the increase of the loss rates due to both absorption and Rayleigh scattering).

As in Ref. [17], the CRDS absorption signal is measured for series of pressure ramps at several fixed spectral points (from 5 to 8 depending on the gas mixture) selected in spectral microwindows minimizing the resonance line contribution (in fact, in the considered spectra region, the resonance line contribution is always large and remains the dominant contribution of the water-related absorption -see below). The chosen spectral points are part of the 29 spectral points used in Ref. [17] for the retrieval of the self-continuum absorption in the same region.

All the recordings are performed with a gas flow produced by a commercial humidity generator (from Omicron Technologies) (see Ref. [27] for a detailed description). The gas sample used for the recordings is a mixture of water vapor with 10,000 ppm molar fraction (i.e. 1%) in either synthetic dry air, N_2 , or O_2 (Alphagaz 2, 99.9995 % purity). Water vapor is produced from deionized liquid water in a temperature-regulated membrane system and then mixed with the carrier gas. The pressure and the gas flow in the gas line are controlled by a pressure controller (Model IQP-700C from Bronkhorst) and a mass flow controller (Area model, FC-R7800 series from Hitachi Metals Ltd.), respectively. The water concentration of the humidified gas is controlled by using the dew point temperature measured directly by the remote head of a precision chilled mirror hygrometer (Model S8000 from Mitchell). A small part of the generated gas flow (typically few tens of sccm) is directed inside the cavity where the pressure is varied between 0 and 750 Torr during the pressure ramps.

Two pressure gauges (10 and 1000 Torr full scale, from MKS Instruments, 0.25% of reading accuracy) are used to monitor continuously the total pressure in the cavity. A temperature sensor (TSic 501 from IST, ± 0.1 K accuracy) fixed on the exter-

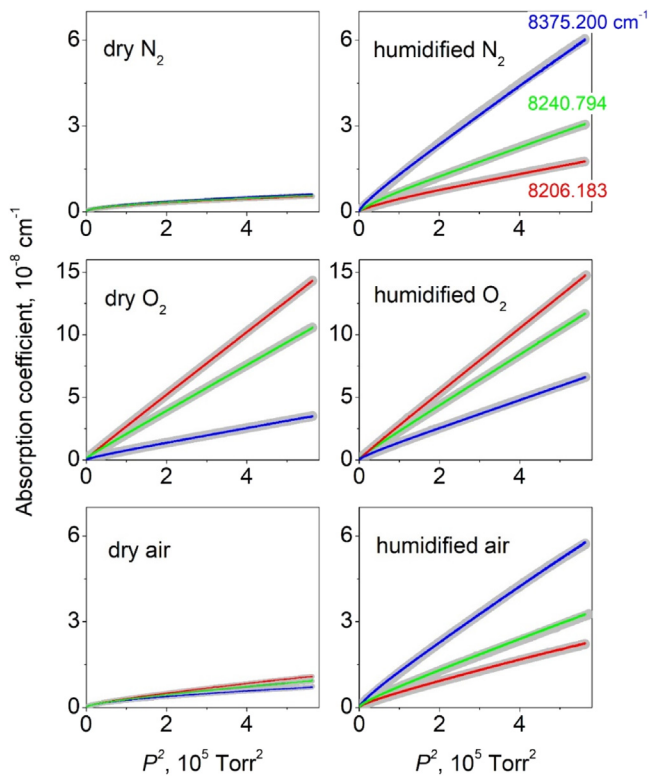


Fig. 1. Variation of the absorption coefficient versus the squared total pressure, P , during pressure ramps up to 750 Torr for three spectral points of the $1.25 \mu\text{m}$ window (8206.183, 8240.794 and 8375.200 cm^{-1} - red, green and blue curves, respectively). For each spectral point, measurements were performed during increasing and decreasing pressure ramps (grey and colored lines, respectively) for dry and humidified gas samples of synthetic air, N_2 and O_2 (left and right panels, respectively). Note the different scale adopted in the case of O_2 .

nal wall of the cavity and enveloped by thermal insulation foam measure the temperature during the recordings. The temperature remains in the $294 \pm 1 \text{ K}$ range during the whole measurement campaign.

The humidified gas recordings include three steps: (i) increasing pressure ramp with a typical speed of 1 Torr/s (i.e. total duration of about 12 minutes), (ii) checking that the water partial pressure in the cell is constant by repetitive scan of a water line during about 1 hour and, (iii) decreasing pressure ramp (about 12 minutes). In addition, just after or just before this recording sequence, an additional recording is performed with the corresponding dry gas sample for an increasing and a decreasing pressure ramp. The dry gas pressure ramps measurements are used as baselines to be subtracted from humidified gas signal (see below).

The variation of the absorption signal during increasing and decreasing pressure ramps with dry and humidified samples are compared on Fig. 1 for three spectral points. This figure deserves several comments: (i) a nearly perfect superposition is observed for increasing and decreasing pressure measurements, illustrating the stability of the experimental setup and allowing to use the averaged data for further analysis, (ii) in the case of the O_2 measurements, the absorption signal is much larger than for air and N_2 (note the different scales used in Fig. 1) as a result of the impact of the broad collision-induced absorption (CIA) of the $a^1\Delta_g - X^3\Sigma_g^-(0-0)$ band centered near 7900 cm^{-1} [28]. This CIA contribution is smaller at high energy which makes the absorption at 8375.200 cm^{-1} smaller than those at 8206.183 and 8240.794 cm^{-1} in the case of O_2 while it is the opposite in the case of air and N_2 .

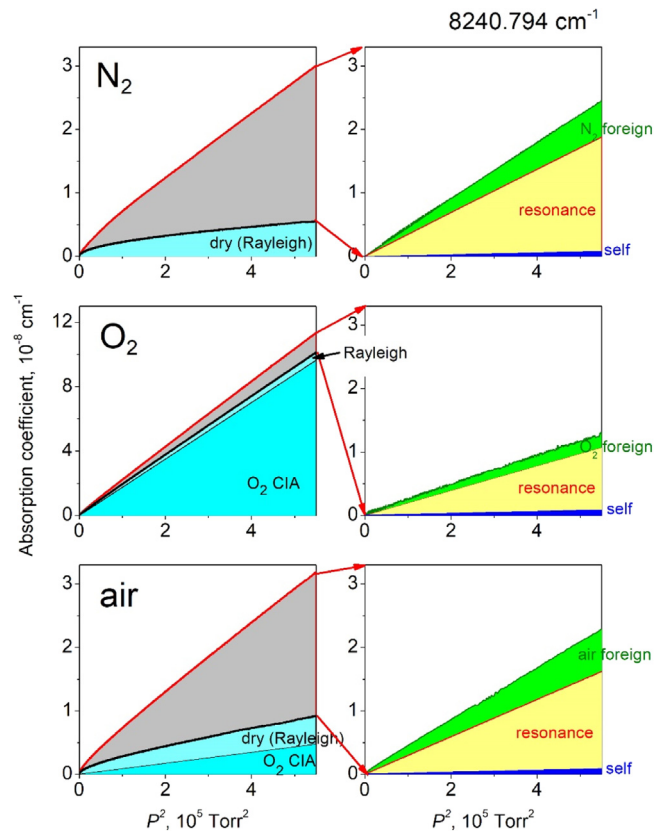


Fig. 2. Left panels: Variation of the absorption coefficient versus the squared total pressure, P , for humidified (red line) and dry (black line) gas samples during pressure ramps up to 750 Torr at the 8240.794 cm^{-1} spectral point. The dry gas “absorption” (cyan background) includes a Rayleigh scattering contribution and a contribution of the CIA of the $1.27 \mu\text{m}$ oxygen band (for O_2 and air). Right panels: The water-related absorption is obtained by difference of the humidified and dry absorption and includes contributions of the water vapor self-continuum absorption (blue area), of the resonance lines, (yellow area) and of the foreign continuum absorption (green area).

3. Cross-section retrieval

On the left panels of Fig. 2, the pressure ramps with humidified and dry gas are superimposed for the 8240.794 cm^{-1} spectral point. The water-related absorption presented on the right panels is obtained by difference. It is important to mention, that the subtraction applies to absorption coefficients corresponding to the same dry gas pressure and not to the same total pressure value. In other words, the water-related absorption measured at a total pressure of $P = P_{\text{H}_2\text{O}} + P_F$ was decreased by the dry gas absorption at P_F . Ignoring the 1% difference between P and P_F in the humidified gas sample would lead to negative water-related absorption in the case of humidified oxygen as 1% of the O_2 CIA is larger than the O_2 foreign continuum absorption of water vapor. This small contribution of the foreign continuum absorption to the measured absorption makes the accurate retrieval of the water foreign continuum absorption particularly challenging in the region.

Let us first consider the dry gas recordings.

Rayleigh scattering is responsible of the variation of the loss rate during the dry N_2 pressure ramps. Rayleigh scattering being proportional to pressure, it leads to a clear curvature for low pressure values when plotted versus pressure squared both for dry and humidified N_2 (Fig. 2 left upper panel). As Rayleigh scattering is mostly identical in the dry and humidified N_2 samples, the curvature nicely vanishes in the water-related contribution obtained by difference and a nearly perfect quadratic dependence versus the

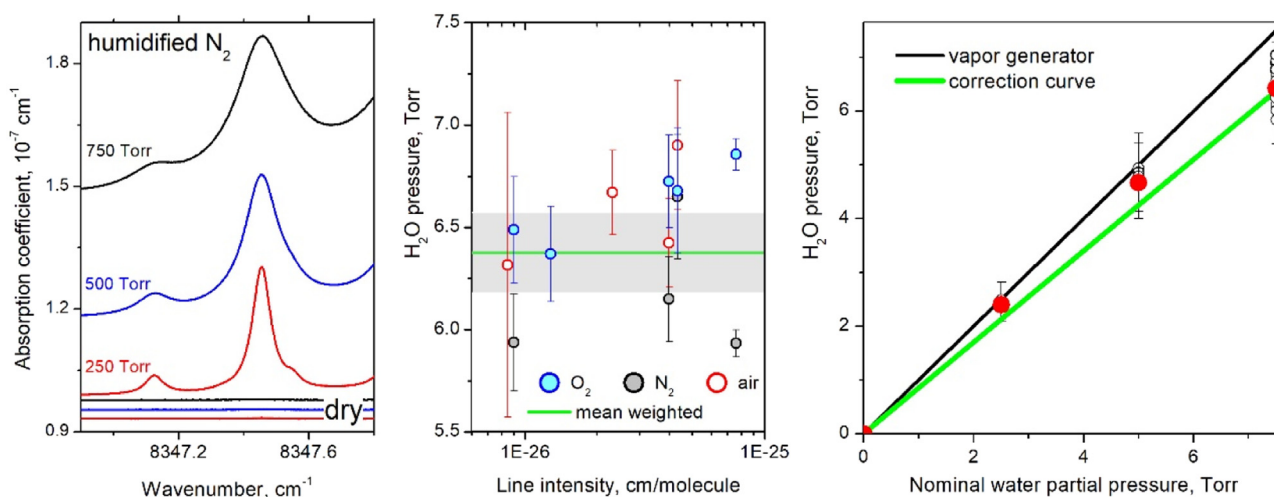


Fig. 3. Left panel: CRDS spectra of 1% humidified N₂ recorded at 250, 500 and 750 Torr total pressures near 8347 cm⁻¹. The three baselines at the bottom of the plot are the corresponding dry N₂ spectra with level increasing linearly with pressure as a consequence of Rayleigh scattering losses.

Middle panel: Water vapor partial pressure values retrieved from a series of recordings of eight lines of water broadened by N₂, O₂ or air at a total pressure of 750 Torr, versus their HITRAN line intensities [30].

Right panel: Water vapor partial pressures retrieved from the line profile analysis versus the nominal partial pressure (1% of the total pressure). The red dots correspond to the line at 8347.46 cm⁻¹ presented on the left panel. The pressure values corresponding to the nominal value at 7.5 Torr are those plotted on the middle panel. The linear fit of the experimental partial pressures versus their nominal values gives a slope of 0.85 (green straight line). This factor was used to correct all the water partial pressure values (see text).

total pressure is achieved (Fig. 2 right upper panel). Indeed, following Eq. 1, the three contributions to the water-related absorption, $\alpha_W(v, T)$, have a pressure squared dependence (the foreign contribution, proportional to $P_{H_2O}P_F$ leads to a P^2 dependence as the mixing ratio of water in the dry gas is fixed to 1%).

Rayleigh scattering contribution of N₂ can be calculated from the refractive index coefficients given in Ref. [29]. The measured losses induced by dry N₂ in our recordings are found to be about 50% larger than expected from calculations. As a check of the calculated values obtained from Ref. [29], we evaluated experimentally the refractive index from the variation of the frequency of the CRDS cavity modes during an increasing pressure ramp of dry N₂ up to 1 atm. 643 modes were counted to scroll during the filling and the evacuating of the cell at a fixed frequency of 8240.794 cm⁻¹. It leads to a refractive index of 1.000279 in perfect agreement with that used in Ref. [29]. The difference between our observations and the calculated Rayleigh scattering losses could be related to mechanical changes in the alignment of the CRDS cell induced by the change of pressure. This effect is believed to have no impact on the retrieval of the water-related continuum absorption as, being reversible (as checked by the consistency of the results obtained with increasing and decreasing pressure ramps), it is cancelled in the subtraction of the humidified N₂ and dry N₂ signals.

In the case of oxygen (Figs. 1 and 2, middle panels), the absorption signal is largely dominated by the CIA. The measured dry O₂ absorption can be compared to calculated values obtained using the CIA binary coefficients of Ref. [28] and the Rayleigh scattering coefficients of Ref. [29]. An excellent agreement (better than 1%) is achieved.

In the case of dry air, the calculated Rayleigh and CIA contributions, highlighted on the lower left panel of Fig. 2, have similar amplitude and our measurements are slightly larger than their predicted sum. As for nitrogen, due to Rayleigh scattering losses, a non-linear dependence on total pressure squared is clearly observed (Fig. 1 lower panels), but after subtraction of the dry part, the water-related absorption pressure dependence becomes nicely linear versus the squared pressure (lower right panel of Fig. 2).

Let us now consider the water-related absorption.

In the considered region corresponding to the high energy edge of the 1.25 μ m transparency window, the resonance line contribution is the dominant part of the water-related absorption. We used the same convention as adopted for the MT_CKD model to simulate the resonance spectrum: line profile was assumed to be of Voigt type and the line wings were truncated at ± 25 cm⁻¹ frequency detuning from the line center, the underlying pedestal being considered as part of the continuum absorption. [Note that the O₂ absorption lines of the 1.27 μ m band are very weak above 8100 cm⁻¹ (intensity smaller than 10⁻²⁹ cm/molecule) and have thus a negligible contribution to the absorption].

A major issue of the current analysis is related to the knowledge of the real water vapor partial pressure in the CRDS cell. Indeed, on the basis of spectra recorded over intervals corresponding to mostly isolated water lines, it appeared that the simulation of the resonance line spectrum calculated using the nominal 10000 ppm relative concentration (corresponding to the set point of the humidity generator) leads to an overestimation of the resonance line absorption. In other words, probably due to adsorption effects in the gas line going to the high finesse cavity, the real water pressure value in the cell is lower than its nominal value. In order to determine its value, eight mostly isolated (broadened) water lines were selected and recorded for total pressure values of humidified gas of 250, 500 and 750 Torr. Fig. 3 shows an example of recorded line (left panel), together with the different retrieved pressure values obtained from the eight lines broadened by O₂, N₂ or air versus their intensities (central panel) and the comparison with the nominal pressure values (right panel). A weighted linear fit of the obtained P_{H_2O} values versus their nominal values (i.e. 1.00 % of the total pressure) was performed. The weight attached to each pressure value was fixed according to its uncertainty calculated as the square root of the quadratic sum of the experimental noise, the fit uncertainty and the HITRAN intensity uncertainty. As a result, the obtained partial pressure in the cell differs from its nominal value by about 15% (green line Fig. 3, right panel). In the following analysis of the recorded pressure ramps, this correction will be applied to all the nominal water vapor partial pressures. In spite of the high signal-to-noise level of the recorded spectra and our careful analysis of about twenty water line recordings, the large

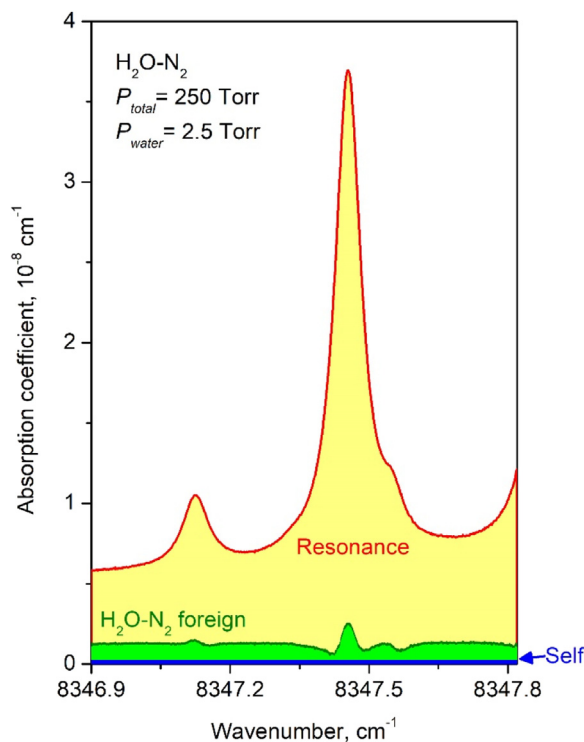


Fig. 4. The different contributions to the water-related absorption in humidified N_2 at a total pressure of 250 Torr, near 8347 cm^{-1} : self-continuum (blue), H_2O-N_2 foreign continuum (green) and resonance line contribution (yellow).

broadening of the line profile makes an accurate determination of the line area difficult (due to baseline uncertainty). As a result, the uncertainty on the amplitude of the pressure correction remains a potential source of uncertainty on the derived foreign cross-section values (see below).

As mentioned above, the water resonance line contribution was simulated as a sum of Voigt line profiles with the standard $\pm 25\text{ cm}^{-1}$ wing cut-off. Line intensities, self- and air-broadening coefficients were taken from the HITRAN2020 database [30]. N_2 - and O_2 -broadening coefficients of water lines are not provided in the HITRAN lists. The water line broadening parameters by N_2 (γ_{N_2}) were calculated in [31] in the frame of MCRB formalism and the “HITRAN” list attached to this work as supplementary material, including γ_{N_2} , was adopted. Oxygen-broadening coefficients of each water line, γ_{O_2} , were calculated using the equation $\gamma_{air} = 0.79\gamma_{N_2} + 0.21\gamma_{O_2}$, using γ_{air} , and γ_{N_2} from HITRAN2020 and Ref. [31], respectively.

The last contribution which has to be subtracted is the water self-continuum (see Eq. 1). It was calculated using the self-continuum cross-section values derived by CRDS of pure water vapor [17]. The different contributions to the water-related absorption are separated on Fig. 4 in a small spectral interval around 8347 cm^{-1} . After the subtraction of the resonance line contribution, significant residuals are obtained near the line centres as a result of some inaccuracies of the line parameters used to compute the resonance line-shape. At the chosen spectral point, the foreign continuum absorption represents less than 20% of the water-related absorption illustrating the difficulty of an accurate evaluation.

On the right panels of Fig. 2, the different contributions are presented for the pressure ramp at 8240.794 cm^{-1} . The self-continuum contribution is small (a few %) while the resonance line contribution represents about 70% of the total absorption. This is a typical situation for all the measurement points listed in Table 1:

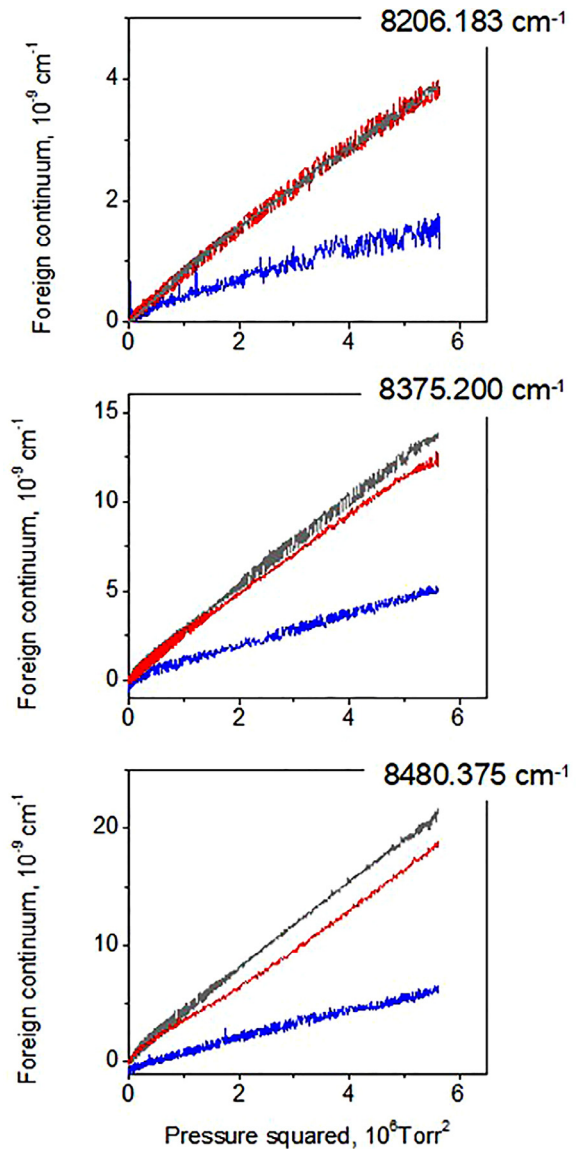


Fig. 5. Variation of the absorption coefficient corresponding to the foreign gas contribution versus the squared total pressure, P , during pressure ramps up to 750 Torr for three spectral points of the $1.25\text{ }\mu\text{m}$ window (8206.183 , 8375.200 and 8480.375 cm^{-1}). Traces in grey, blue and red correspond to gas samples of humidified (10000 ppm) N_2 , O_2 and synthetic air, respectively. Each curve corresponds to the measured absorption signal decreased by the dry gas contribution, the resonance gas contribution and the water self-continuum and is the superposition of the increasing and decreasing pressure ramps.

in spite of a careful selection of microwindows minimizing the resonance line contribution, the latter represents most of the water-related absorption at all measurement points. The relative contribution of the resonance line to the water-related absorption (ranging between 61 and 83%) is given in Table 1 for each spectral point.

The pressure dependence of the water-related absorption after subtraction of the self-continuum and resonance lines contributions is presented in Fig. 5 for air, N_2 and O_2 pressure ramps at three measurement points. A good pressure squared dependence is achieved as expected from Eq. 1 (recall that P_{H_2O} and P are proportional). Note that the plotted ramps are in fact the superposition of the increasing and decreasing pressure ramp signals. The foreign continuum cross-sections listed in Table 1 were obtained from a linear fit of the pressure dependences using Eq. 1.

Table 1Foreign gas cross-sections of water vapor (C_F) derived at nine spectral points between 8100 and 8500 cm^{-1} .

Wavenumber, cm^{-1}	C_F $10^{-27} \text{ cm}^2 \text{ molecule}^{-1} \text{ atm}^{-1}$			Resonance absorption %			Uncertainty due to resonance spectrum $10^{-27} \text{ cm}^2 \text{ molecule}^{-1} \text{ atm}^{-1}$		
	N_2	O_2	air	N_2	O_2	air	N_2	O_2	air
8105.865	-	5.3(3)	-	-	49.6	-	-	2.1	-
8123.155	7.6(1.1)	0.3(2)	3.8(9)	68.6	82.6	77.0	2.3	3.8	4.4
8206.183	19(2)	7.7(8)	19.1(1.9)	63.1	67.2	61.3	4.1	6.3	7.6
8240.794	33(4)	10.1(1.9)	33.0(3.7)	69.8	77.7	67.6	8.8	14.2	16.9
8279.585	-	-	53.5(7.0)	-	-	72.4	-	-	34.3
8317.615	-	26.7(4.7)	-	-	76.1	-	-	32.3	-
8375.200	68.2(8.5)	25.9(5.1)	62.0(8.0)	71.4	78.0	71.8	14.3	33.8	32.3
8434.240	-	52.1(6.9)	-	-	68.8	-	-	40.2	-
8480.505	104(11)	33.3(6)	88.4(10.0)	66.5	74.2	67.8	12.9	37.5	42.0

Notes

Columns 2-4: C_F values for N_2 , O_2 and air, respectively, with corresponding experimental uncertainty given between parenthesis. The uncertainty value is limited to the statistical fit uncertainty and water partial pressure uncertainty.

Columns 5-7: Corresponding fraction (in %) of the resonance absorption contribution to the water-related absorption.

Columns 8-10: Uncertainty related to the subtraction of the resonance absorption contribution evaluated on the basis of the errors on the HITRAN line parameters.

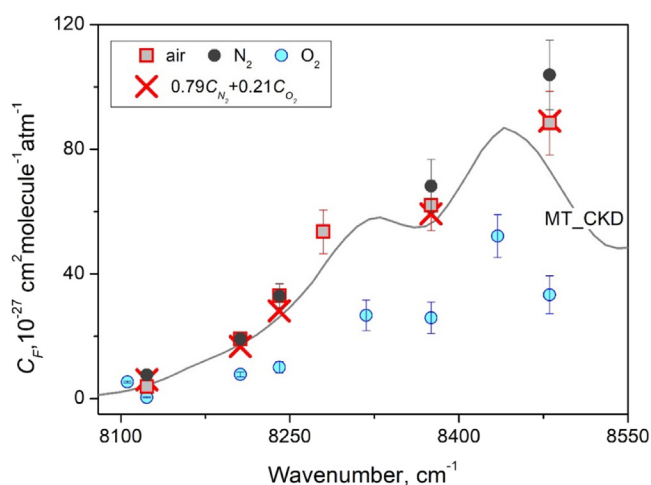


Fig. 6. Overview of the foreign continuum cross-sections, C_F , retrieved for N_2 (black dots), O_2 (blue dots) and dry air (red squares) between 8100 and 8500 cm^{-1} and comparison to the values provided for air by the MT_CKD_V3.5. The red crosses correspond to the calculated values of C_{air} obtained from $C_{\text{air}} = 0.79C_{\text{N}_2} + 0.21C_{\text{O}_2}$. The plotted error bars are those given in Columns 2-4 of Table 1 and are limited to the combined impact of the uncertainty on the water partial pressure (about 3%) and on the linear coefficient of the pressure ramp fit (see Text).

4. Discussion and concluding remarks

Fig. 6 shows an overview of the retrieved foreign cross-sections. The plotted error bars are limited to the experimental uncertainties on the (corrected) value of the water partial pressure (about 3%), and on the linear coefficient of the pressure ramp fit (on the order of 1 % for N_2 and O_2 and up to 15% for air). It should be pointed that the above 15 % correction of the partial pressure of water in the cell has an important impact on the obtained C_F values. In absence of correction, C_{N_2} and C_{air} values would have been smaller by a factor 2-3 while the C_{O_2} cross-sections would have been decreased to a level too weak to be evaluated.

As in the retrieval of the water self-continuum cross-sections in the same region [17], an additional important error source should be considered. It is related to the evaluation of the resonance line contribution which represents 60-80% of the water-related absorption and has thus a strong impact on the retrieved C_F values. In other words, the obtained C_F values cannot be dissociated from the resonance line databases we used for their retrieval. Based on the error codes attached to the HITRAN line parameters [30], we evaluated the uncertainty on the resonance line contribution. The

obtained error bars included in Table 1 are sometimes comparable to our absolute C_F values. This problematic situation may indicate that our obtained C_F values should be used with much caution or/and that the HITRAN error bars are overestimated. There is some indication that HITRAN uncertainties on the broadening parameters are indeed overestimated: in the case of N_2 , the uncertainties on the resonance line contribution included in Table 1 were obtained from the “HITRAN” list produced by Vispoel et al. [31] (where error values are attached to each N_2 -broadening coefficient instead of error codes given in HITRAN for air-broadening coefficients). As a result, the obtained resonance line uncertainties are 2-3 times smaller for N_2 than for air (see Table 1).

In spite of the doubts on the estimation of the error bars, a number of observations give some confidence to our results:

- The overall consistency between the C_{N_2} and C_{air} values, determined independently, is very good, the C_{N_2} values being generally larger than C_{air} values,
- Air foreign continuum cross-sections calculated as $C_{\text{air}} = 0.79C_{\text{N}_2} + 0.21C_{\text{O}_2}$ (red crosses in Fig. 6) nicely agree with the direct experimental determinations of C_{air} (red squares) illustrating the self-consistency of three sets of measurements: C_{O_2} values being smaller than C_{N_2} and C_{air} values, the differences between C_{N_2} and C_{air} values are close to the calculated impact of the O_2 contribution on C_{air} values,
- The comparison of experimental and calculated C_{air} values with the MT_CKD model shows an overall good agreement. We also note that C_{O_2} frequency dependence is consistent with the two maxima of the MT_CKD model.

From Table 1 and Fig. 6, it appears that the foreign cross-sections are significantly smaller for O_2 than for N_2 . In the literature, the dependence of the water foreign continuum upon the nature of the foreign gas has been rarely discussed. In several experimental studies using N_2 as foreign gas, the obtained water- N_2 cross-sections are compared to the MT_CKD model (which is for air) with the implicit assumption that water- O_2 and water- N_2 cross-sections are close. In fact, little is known on the water- O_2 foreign continuum. To the best of our knowledge, the only previous study which reported water foreign cross-section for O_2 , N_2 and air was performed in the far infrared (FIR) [32]. Although the strong resonance line contribution was a limiting factor of the analysis (as in the present study), the water- O_2 continuum in the rotational region (50-700 cm^{-1}) was found largely smaller than the water- N_2 and water-air continua (in fact, C_{O_2} appeared to be too weak to be experimentally determined i.e. more than five times smaller than, C_{N_2} and C_{air} – see Fig. 6 of Ref. [32]). Here, the measure-

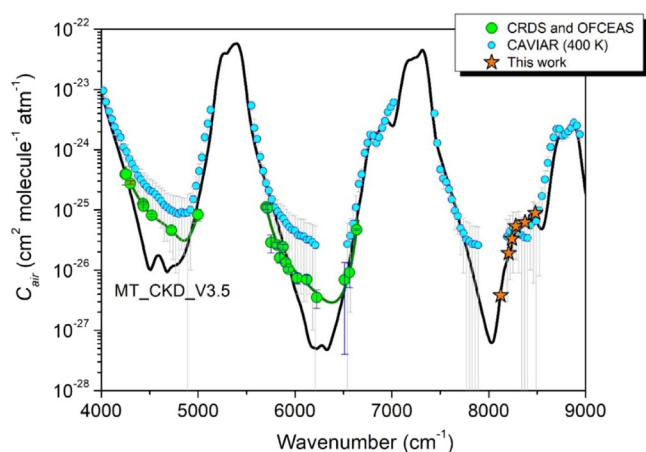


Fig. 7. Overview of the water foreign continuum cross-sections, C_{air} between 4000 and 9000 cm^{-1} obtained in this work and found in the literature [9,14,15,21], and comparison to the MT_CKD_V3.5 model. The CAVIAR experimental values [21] were obtained at 400 K while the other displayed values correspond to the room temperature.

ment of the water- O_2 continuum is made even more challenging due to the overlapping with the CIA band of O_2 near 1.27 μm . At the 8240.794 cm^{-1} spectral point of Fig. 2, the water-related absorption represents about 10% of the measured absorption and the O_2 -foreign itself no more than 1.6 % which obliges to some caution when considering the derived C_{O_2} values. Nevertheless, the obtained frequency dependence of C_{O_2} appears to be reasonable which gives some credit to the evidenced smaller amplitude of the water- O_2 continuum compared to the water- N_2 continuum. Although the oxygen concentration in air is only 21%, the resulting decrease of the water-air continuum compared to the water- N_2 continuum is consistent with the observations (see Fig. 6).

Note that in the frame of the far wings interpretation of the water foreign continuum, the water- O_2 and the water- N_2 continua are expected to scale according to the corresponding water broadening coefficients. Roughly, the broadening coefficients of water lines by O_2 are on average 30% smaller than those by N_2 . This factor appears to be not far from the scaling factor of the C_{O_2} and C_{N_2} cross-sections determined in the present work but disagrees with the FIR observations [32].

We have gathered in Fig. 7, the room temperature water-air foreign cross-sections derived in this work and in our previous CRDS studies in the 2.3 and 1.6 μm windows [9,14,15], and compared them to the MT_CKD_V3.5 foreign continuum. A clear underestimation of the MT_CKD model was evidenced in the 2.3 and 1.6 μm windows, which is not the case in the presently studied 1.25 μm window where the MT_CKD model is validated. The foreign (air) cross-sections reported by the CAVIAR consortium [21] have been superimposed on the plot. The CAVIAR measurements by FTS were performed at 350, 372, 402 and 431 K (which allowed to increase the absorption signal by increasing the water partial pressure to a few hundreds of mbar). In the 1.25 μm window, the large (1σ) error bars of the CAVIAR measurements (on the order of 100%) do not allow for a sound comparison. Nevertheless, the order of magnitude of CAVIAR C_{air} values at 400 K is reasonable compared to our room temperature measurements (let us recall that the temperature dependence of the foreign continuum is known to be very weak).

As a final conclusion, the first (challenging) measurements of the air-, O_2 -, and N_2 -water continua at room temperature have been performed in the 1.25 μm window from a series of pressure ramps at fixed spectral points. The humidity rate was fixed to 1% and the measured total continuum absorption were found to fol-

low satisfactorily the expected quadratic dependence *versus* the total pressure up to 1 atm. In spite of the sensitivity and stability of the used CRDS setup (illustrated by the obtained pressure squared dependences), the accuracy of our final cross-section values is limited. As the foreign continuum represents a small fraction of the measured absorption signal and as some of the other contributions (far wings of the resonance lines, O_2 collision induced absorption, self-continuum, Rayleigh scattering) are known with large uncertainties (e.g. resonance line absorption), we cannot claim a high accuracy on the reported cross-section values. In addition, the real humidity rate in the CRDS cell had to be estimated from a line profile analysis which led to a correction of 15% compared to its nominal value. As a result, we roughly estimate to 50% the overall error bars on our cross-section values. The agreement with the MT_CKD model, unexpectedly better than this error bar, might be coincidental. We thus conclude that in the 1.27 μm transparency window, the MT_CKD model is validated within our uncertainties, which was not the case in the 2.3 and 1.6 μm windows, where an underestimation of the MT_CKD values by up to a factor 10 were measured in the centers of the windows [9,14,15].

The question of the relative amplitude of the O_2 -, and N_2 -water continua deserves further investigation in more favorable spectral ranges. The 1.6 μm window is considered for dedicated study of this issue.

Declaration of Competing Interest

The authors declare that they have no known competing financial interests or personal relationships that could have appeared to influence the work reported in this paper.

CRediT authorship contribution statement

A.O. Koroleva: Investigation. **S. Kass:** Investigation. **D. Mondelain:** Investigation. **A. Campargue:** Investigation.

Data availability

Data will be made available on request.

Acknowledgements

This project is supported by the French National Research Agency in the framework of the "Investissements d'avenir" program (ANR-15-IDEX-02) and by CNRS (France) in the frame of the International Research Project "SAMIA". We would like to thank Robert Gamache (University of Massachusetts Lowell) for valuable discussion about the water broadening coefficients by N_2 and O_2 .

References

- [1] Clough SA, Kneizys FX, Davies RW. Line shape and the water vapor continuum. *Atm Res* 1989;23:229–41. doi:10.1016/0169-8095(89)90020-3.
- [2] Mlawer EJ, Payne VH, Moncet J, Delamere JS, Alvarado MJ, Tobin DC. Development and recent evaluation of the MT_CKD model of continuum absorption. *Phil Trans R Soc A* 2012;370:2520–56. doi:10.1098/rsta.2011.0295.
- [3] https://github.com/AER-RC/MT_CKD/
- [4] Burch DE. Continuum absorption by H_2O . Report AFGL-TR-81-0300, Air Force Geophys. Laboratory, Hanscom AFB, MA, 1982.
- [5] Burch DE, Alt RL. Continuum absorption by H_2O in the 700–1200 cm^{-1} and 2400–2800 cm^{-1} windows. Report AFGL-TR-84-0128, Air Force Geophys. Laboratory, Hanscom AFB, MA, 1984.
- [6] Burch DE. Absorption by H_2O in narrow windows between 3000 and 4200 cm^{-1} . Report AFGL-TR-85-0036, Air Force Geophys. Laboratory, Hanscom AFB, MA, 1985.
- [7] Mondelain D, Aradj A, Kass S, Campargue A. The water vapor self-continuum by CRDS at room temperature in the 1.6 μm transparency window. *J Quant Spectrosc Radiat Transfer* 2013;130:381–91. doi:10.1016/j.jqsrt.2013.07.006.
- [8] Mondelain D, Manigand S, Manigand S, Kass S, Campargue A. Temperature dependence of the water vapor self-continuum by cavity ring-down spectroscopy in the 1.6 μm transparency window. *J Geophys Res Atmos* 2014;119(9):2169–8996. doi:10.1002/2013JD021319.

- [9] Mondelain D, Vasilchenko S, Čermák P, Kass S, Campargue A. The self- and foreign-absorption continua of water vapor by cavity ring-down spectroscopy near 2.35 μm . *Phys Chem Chem Phys* 2015;17(762–17):770–17. doi:[10.1039/c5cp01238d](https://doi.org/10.1039/c5cp01238d).
- [10] Ventrillard I, Romanini D, Mondelain D, Campargue A. Accurate measurements and temperature dependence of the water vapor self-continuum absorption in the 2.1 μm atmospheric window. *J Chem Phys* 2015;143:134304. doi:[10.1063/1.4931811](https://doi.org/10.1063/1.4931811).
- [11] Campargue A, Kass S, Mondelain D, Vasilchenko S, Romanini D. Accurate laboratory determination of the near infrared water vapor self-continuum: A test of the MT_CKD model. *J Geophys Res Atmos* 2016;121(13) 180–13203. doi:[10.1002/2016JD025531](https://doi.org/10.1002/2016JD025531).
- [12] Richard L, Vasilchenko S, Mondelain D, Ventrillard I, Romanini D, Campargue A. Water vapour self-continuum absorption measurements in the 4.0 and 2.1 μm transparency windows. *J Quant Spectrosc Radiat Transf* 2017;201:171–9. doi:[10.1016/j.jqsrt.2017.06.037](https://doi.org/10.1016/j.jqsrt.2017.06.037).
- [13] Lechevallier L, Vasilchenko S, Grilli R, Mondelain D, Romanini D, Campargue A. The water vapour self-continuum absorption in the infrared atmospheric windows: new laser measurements near 3.3 and 2.0 μm . *Atmos Meas Tech* 2018;11:2159–71. doi:[10.5194/amt-11-2159-2018](https://doi.org/10.5194/amt-11-2159-2018).
- [14] Vasilchenko S, Campargue A, Kass S, Mondelain D. The water vapour self- and foreign-continua in the 1.6 μm and 2.3 μm windows by CRDS at room temperature. *J Quant Spectrosc Radiat Transfer* 2019;227:230–8. doi:[10.1016/j.jqsrt.2019.02.01](https://doi.org/10.1016/j.jqsrt.2019.02.01).
- [15] Mondelain D, Vasilchenko S, Kass S, Campargue A. The water vapor foreign-continuum in the 1.6 μm window by CRDS at room temperature. *J Quant Spectrosc Radiat Transfer* 2020;246:106923. doi:[10.1016/j.jqsrt.2020.106923](https://doi.org/10.1016/j.jqsrt.2020.106923).
- [16] Fleurbaey H, Grilli R, Mondelain D, Campargue A. Measurements of the water vapor continuum absorption by OFCEAS at 3.50 μm and 2.32 μm . *J Quant Spectrosc Radiat Transf* 2022;278:108004. doi:[10.1016/j.jqsrt.2021.108004](https://doi.org/10.1016/j.jqsrt.2021.108004).
- [17] Koroleva AO, Kass S, Campargue A. The water vapor self-continuum absorption at room temperature in the 1.25 μm window. *J Quant Spectrosc Radiat Transf* 2022;286:108206. doi:[10.1016/j.jqsrt.2022.108206](https://doi.org/10.1016/j.jqsrt.2022.108206).
- [18] Hartmann J-M, Tran H, Armante R, Boulet C, Campargue A, Forget F, Gianfrani L, Gordon I, Guerlet S, Gustafsson M, Hodges JT, Kass S, Lisak D, Thibault F, Toon GC. Recent advances in collisional effects on spectra of molecular gases and their practical consequences. *J Quant Spectrosc Radiat Transfer* 2018;213:178–227. doi:[10.1016/j.jqsrt.2018.03.016](https://doi.org/10.1016/j.jqsrt.2018.03.016).
- [19] Paynter D J, Ptashnik I V, Shine K P, Smith K M, McPheat R, Williams R G. Laboratory measurements of the water vapour continuum in the 1200–8000 cm^{-1} region between 293K and 351 K. *J Geophys Res* 2009;114:D21301. doi:[10.1029/2008JD011355](https://doi.org/10.1029/2008JD011355).
- [20] Reichert L, Andrés Hernández MD, Burrows JP, Tikhomirov AB, Firsov KM, Ptashnik IV. First CRDS-measurements of water vapour continuum in the 940 nm absorption band. *J Quant Spectrosc Radiat Transf* 2007;105:303–11. doi:[10.1016/j.jqsrt.2006.10.010](https://doi.org/10.1016/j.jqsrt.2006.10.010).
- [21] Ptashnik IV, McPheat RA, Shine KP, Smith KM, Williams RG. Water vapour foreign-continuum absorption in near-infrared windows from laboratory measurements. *Phil Trans R Soc A* 2012;370:2557–77. doi:[10.1098/rsta.2011.0218](https://doi.org/10.1098/rsta.2011.0218).
- [22] Baranov YI. The continuum absorption in $\text{H}_2\text{O}+\text{N}_2$ mixtures in the 2000–3250 cm^{-1} spectral region at temperatures from 326 to 363 K. *J Quant Spectrosc Radiat Transfer* 2011;112:2281–6. doi:[10.1016/j.jqsrt.2011.06.005](https://doi.org/10.1016/j.jqsrt.2011.06.005).
- [23] Baranov YI, Buryak IA, Lokshantov SE, Lukyanenko VA, Vigasin AA. $\text{H}_2\text{O}-\text{N}_2$ collision-induced absorption band intensity in the region of the N_2 fundamental: ab initio investigation of its temperature dependence and comparison with laboratory data. *Phil Trans R Soc A* 2012;370:2691–709. doi:[10.1098/rsta.2011.0189](https://doi.org/10.1098/rsta.2011.0189).
- [24] Baranov YI, Lafferty WJ. The water vapour self- and water-nitrogen continuum absorption in the 1000 and 2500 cm^{-1} atmospheric windows. *Phil Trans R Soc A* 2012;370:2578–89. doi:[10.1098/rsta.2011.0234](https://doi.org/10.1098/rsta.2011.0234).
- [25] Cormier JG, Hodges JT, Drummond JR. Infrared water vapor continuum absorption at atmospheric temperatures. *J Chem Phys* 2005;122:114309. doi:[10.1063/1.1862623](https://doi.org/10.1063/1.1862623).
- [26] Tikhomirov AB, Ptashnik IV, Tikhomirov BA. Measurements of the continuum absorption coefficient of water vapour near 14400 cm^{-1} (0.694 μm). *Opt Spectrosc* 2006;101:80.
- [27] Fleurbaey H, Campargue A, Carreira Mendès Da Silva Y, Grilli R, Kass S, Mondelain D. Characterization of the $\text{H}_2\text{O}+\text{CO}_2$ continuum within the infrared transparency windows. *J Quant Spectrosc Radiat Transf* 2022;282:108119. doi:[10.1016/j.jqsrt.2022.108119](https://doi.org/10.1016/j.jqsrt.2022.108119).
- [28] Mondelain D, Kass S, Campargue A. Accurate laboratory measurement of the O_2 collision-induced absorption band near 1.27 μm . *J Geophys Res Atmos* 2018;124(1):414–23. doi:[10.1029/2018JD029317](https://doi.org/10.1029/2018JD029317).
- [29] Thalman R, Zarzana K, Tolbert MA, Volkamer R. Rayleigh scattering cross-section measurements of nitrogen, argon, oxygen and air. *J Quant Spectrosc Radiat Transf* 2014;147:171–7. doi:[10.1016/j.jqsrt.2014.05.030](https://doi.org/10.1016/j.jqsrt.2014.05.030).
- [30] Gordon IE, Rothman LS, Hargreaves RJ, Hashemi R, Karlovets EV, Skinner FM, et al. The HITRAN2020 molecular spectroscopic database. *J Quant Spectrosc Radiat Transf* 2022;277:107949. doi:[10.1016/j.jqsrt.2021.107949](https://doi.org/10.1016/j.jqsrt.2021.107949).
- [31] Vispoel B, Cavalcanti JH, Paige ET, Gamache RR. Vibrational dependence, temperature dependence, and prediction of line shape parameters for the $\text{H}_2\text{O}-\text{N}_2$ collision system. *J Quant Spectrosc Radiat Transf* 2020;253:107030. doi:[10.1016/j.jqsrt.2020.107030](https://doi.org/10.1016/j.jqsrt.2020.107030).
- [32] Koroleva AO, Odintsova TA, MYu Tretyakov, Pirali O, Campargue A. The foreign-continuum absorption of water vapour in the far-infrared (50–500 cm^{-1}). *J. Quant. Spectrosc. Rad. Transf.* 2021;261:107486.